Proteomics of isolated sieve tubes from *Nicotiana tabacum*: sieve element–specific proteins reveal differentiation of the endomembrane system

Yan Liu[a,1], Viktoriya V. Vasina[a,1], Max E. Kraner[b], Winfried S. Peters[a,c], Uwe Sonnewald[b], and Michael Knoblauch[a,2]

[a]School of Biological Sciences, Washington State University, Pullman, WA 99154; [b]Division of Biochemistry, Department of Biology, Friedrich-Alexander-University Erlangen-Nuremberg, 91058 Erlangen, Germany; and [c]Department of Biology, Purdue University Fort Wayne, Fort Wayne, IN 46835

Edited by Patricia Zambryski, Department of Plant and Microbial Biology, University of California, Berkeley, CA; received July 13, 2021; accepted November 18, 2021

Symplasmicly connected cells called sieve elements form a network of tubes in the phloem of vascular plants. Sieve elements have essential functions as they provide routes for photoassimilate distribution, the exchange of developmental signals, and the coordination of defense responses. Nonetheless, they are the least understood main type of plant cells. They are extremely sensitive, possess a reduced endomembrane system without Golgi apparatus, and lack nuclei and translation machineries, so that transcriptomics and similar techniques cannot be applied. Moreover, the analysis of phloem exudates as a proxy for sieve element composition is marred by methodological problems. We developed a simple protocol for the isolation of sieve elements from leaves and stems of *Nicotiana tabacum* at sufficient amounts for large-scale proteome analysis. By quantifying the enrichment of individual proteins in purified sieve element relative to bulk phloem preparations, proteins of increased likelyhood to function specifically in sieve elements were identified. To evaluate the validity of this approach, yellow fluorescent protein constructs of genes encoding three of the candidate proteins were expressed in plants. Tagged proteins occurred exclusively in sieve elements. Two of them, a putative cytochrome b561/ferric reductase and a reticulon-like protein, appeared restricted to segments of the endoplasmic reticulum (ER) that were inaccessible to green fluorescent protein dissolved in the ER lumen, suggesting a previously unknown differentiation of the endomembrane system in sieve elements. Evidently, our list of promising candidate proteins (*SI Appendix*, Table S1) provides a valuable exploratory tool for sieve element biology.

phloem | proteomics | sieve element | sieve tube endomembrane system

Organic substances serving as materials and energy sources for humans and terrestrial life generally originate from photosynthesis in vascular plants. In these autotrophs, products of photosynthesis are transported from photosynthetic source organs to distant sinks, where they drive growth and development or are stored for later usage (1–4). Photoassimilate translocation proceeds as bulk flow in the sieve tubes of the phloem. Sieve tubes are coherent arrays of cells called sieve elements, which in angiosperms form symplasmic units with adjacent companion cells (5–7). Immature sieve elements turn the cell walls between them into the characteristic sieve plates through partial resorption and disband vacuoles, Golgi apparatus, cytoskeleton, and nuclei to create a network of continuous tubes of low hydraulic resistance (7–9). In addition to the moving, photoassimilate-rich cytosol, active sieve elements contain stationary, peripheral endoplasmic reticulum and mitochondria, as well as sieve element plastids and phloem-specific or P-proteins of obscure functional significance (10–12). With gene expression being impossible in mature sieve elements, any functional proteins in these cells must either have been imported or represent remainders of translational activities in undifferentiated sieve element precursor cells (13). In the latter case, the proteins have to remain functional for the lifetime of the sieve elements.

Our current understanding of the roles sieve tube components such as plastids and P-proteins play in phloem function is lamentably poor, for which there are two main reasons. The first one is exemplified by a recent large-scale study that revealed the "distinct identities of leaf phloem cells by single cell transcriptomics" (14). In fact, all vascular cell types were characterized, except for sieve elements—hardly surprising, as analyses of gene activity and protein synthesis cannot elucidate the function(s) of cells that lack nuclei and translation machineries. The second problem is the notorious noncooperativeness of sieve elements as study objects (11, 12, 15). Functional tubes are hard to observe, as they contribute only a small proportion of the vascular tissues and are embedded in multiple layers of other cell types (5). Because active tubes form symplasmic networks that are under high turgor pressure (16), the excision of organs or tissue segments for detailed investigation causes immediate cessation of sieve tube function. For the same reason, any tissue wounding induces structural artifacts in the entire system (17), such as the deposition of proteinaceous slime on sieve plates

Significance

Sieve elements are crucially important plant cells that distribute photoassimilates and communicate developmental and defensive signals throughout the plant body. They remain the least understood cell type in plants nonetheless, defying standard research methods as they are exceedingly sensitive and possess neither nucleus (no DNA) nor protein synthesis. We developed a protocol to isolate sieve elements for proteome analysis and discovered unfamiliar sieve element–specific proteins that define an internal differation of the endoplasmic reticulum—which demonstrates the power of this approach to the elusive sieve element.

Author contributions: M.K. and U.S. designed and coordinated the project; M.K. developed sieve tube isolation methods; M.E.K. performed mass spectrometry and prepared the results for further analysis by W.S.P.; Y.L. and V.V.V. isolated tissue samples, generated and analyzed transgenic plants; M.K. performed FRAP experiments; and W.S.P. wrote the manuscript with input from Y.L., which was discussed, improved, and finally approved by all authors.

The authors declare no competing interest.

This article is a PNAS Direct Submission.

[1]Y.L. and V.V.V. contributed equally to this work.

[2]To whom correspondence may be addressed. Email: knoblauch@wsu.edu.

This article contains supporting information online at http://www.pnas.org/lookup/suppl/doi:10.1073/pnas.2112755119/-/DCSupplemental.

Published December 30, 2021.

(18, 19), the "explosion" of sieve element plastids (19), and the constriction of sieve tubes by cell wall swelling (20).

Severed vascular tissues of several species expel fluid, in some cases over prolonged periods. These exudates, presumed equivalents of the fluids flowing through the sieve tubes of the living plant, can be collected and analyzed (21). Numerous investigations into the composition of exudates have focused on proteins (e.g., refs. 22–29), but the interpretation of the results is complicated by two problems. First, because injuries inflicted to provoke phloem exudation always affect a variety of cell types, exudates cannot be expected to be pure. Significant portions of the "phloem exudates" collected from the frequently studied cucurbits were reported to originate from nonphloem cells (30). Similarly, exudates from *Arabidopsis* were found to contain proteins with known functions in the cell wall, "demonstrating contamination of the exudate" (27). Second, even if the assumption of an exclusive sieve element origin for a given exudate protein were reasonable, the protein's presence in exudates would not necessarily imply a physiological function in these cells (31). For example, phloem exudates often contain G-actin [monomeric actin (24−27)], although there is no convincing evidence for an actin-based cytoskeleton operating in mature sieve elements (13). Therefore, the occurrence of G-actin in sieve tubes is explained best by the leakage of this ubiquitous protein into transporting tubes from companion cells and differentiating, immature sieve elements (13, 24). Similarly, the detection in phloem exudates of proteins known to function in translation prompted the conclusion that "protein synthesis likely occurs within the angiosperm phloem translocation stream" (22). However, subsequent studies indicated that the observed ribosomal fragments rather represented molecular debris from the breakdown of the protein synthesis machinery in differentiating sieve element precursor cells (29).

A different problem is that even the purest exudates deliver an incomplete picture of the composition of sieve elements at best because nonsoluble cellular components seem to never join the exuding fluid (32). For example, sieve elements in leguminous plants harbor contractile forisomes, protein bodies that may occlude the tubes reversibly in a Ca^{2+}-dependent fashion (33, 34). Forisomes consist of SEO (sieve element occlusion) proteins (35). No traces of these proteins were detected in phloem exudates from two legumes, *Lupinus albus* (26) and *Lupinus texensis* (28), although forisomes have been documented in seven *Lupinus* spp., including *L. albus* (36). The similar but noncontractile SEOR (SEO-related) proteins are common and often abundant P-proteins in angiosperms including legumes, cucurbits, and model species such as *Populus trichocarpa* and *Arabidopsis* (12, 35, 37, 38). Nonetheless, SEORs are conspicuously absent from phloem exudates; we are aware of only one detection of apparent SEOR proteins, namely several putative homologs of the *Arabidopsis* SEOR1 (At3G01680) in exudates from *Cucurbita maxima* (supplemental table 1 in ref. 21).

Some disadvantages of using exudates to study phloem proteins could be minimized if it were possible to isolate and purify sieve tubes. In fact, the comparison of the protein contents of assumed phloem exudates on one hand and that of microsurgically isolated fascicular phloem on the other has been instrumental in clarifying that the two anatomically distinguishable phloem types of the cucurbits, fascicular and extrafascicular phloem, are physiologically distinct (39, 40). In one of these studies (40), several putative homologs of the two *Arabidopsis* SEOR proteins (At3G01670 and At3G01680) were detected in the fascicular phloem of both *C. maxima* and *Cucumis sativus*. This suggests that phloem isolation by microdissection might enable the recovery of sieve element proteins that are absent from phloem exudates.

We reasoned that macroscopic procedures enabling the preparation of comparatively large amounts of isolated sieve elements could facilitate the application of large-scale proteomics analysis to these cells. We developed methods for the production of isolated phloem as well as purified sieve element samples of over 40 µg from *Nicotiana tabacum* stems and leaves, enabling the identification of proteins enriched in sieve elements compared to bulk phloem. Here, we demonstrate the feasibility of our approach by identifying sieve element–specific proteins through which a previously unknown (sub)compartment of the reduced endomembrane system of these cells can be defined.

Results

Tissue Preparation. In preliminary tests of a variety of species, we had found *N. tabacum* particularly well suited for the manual isolation of large amounts of phloem tissues from stems as well as leaves (*SI Appendix*, Fig. S1). Using an *N. tabacum* line expressing GFP (green fluorescent protein) targeted to the ER (endoplasmic reticulum) by the HDEL retention signal specifically in sieve tubes (pMtSEO2-HDEL-GFP; Fig. 1*A*) enabled the identification of sieve elements throughout the preparation procedure. This facilitated the development of a cell type–specific enzymatic degradation protocol for the purification of sieve elements from bulk phloem preparations (Fig. 1 *B–D*). As a result, we could produce bulk phloem and sieve element samples from both stems and leaves that were sufficient for large-scale comparative proteome analyses. The ability to quantitatively compare the proteomes of bulk phloem and purified sieve elements was essential for our further analyses, in which we aimed at identifying proteins with specific roles in sieve elements through their relative enrichment in purified sieve element preparations.

Proteome Analysis. We analyzed our samples by three-stage mass spectrometry (MS^3) and identified proteins using the protein database derived from the *N. tabacum* reference genome (41), available at https://solgenomics.net. The analysis of three biological replicates each of bulk phloem and sieve element preparations from leaves and stems yielded 3,573 (leaf) and 6,419 (stem) unambiguously identified proteins (complete lists in Dataset S1). Because 2,894 proteins were present in both organs, the total count was 7,098 (Fig. 1*E*). Reproducibility of detection was high; counting protein numbers individually for the four treatments (stem or leaf, bulk phloem or purified sieve elements), the detected protein was found in all three biological replicates in 92.5% of the cases. The vast majority of proteins, 98.3% in leaves and 97.8% in stems, were detectable in both bulk phloem and purified sieve elements (Fig. 1*E*). The differences between bulk phloem and purified sieve elements in the amounts of 35.3% (leaves) and 35.8% (stems) of these proteins were considered insignificant ($P > 0.05$; Student's t test, two-tailed, unequal variance). Of those proteins showing more substantial differences between bulk phloem and sieve element preparations ($P \leq 0.05$), minorities of 28.1% in leaves and only 13.8% in stems were enriched in sieve elements (Fig. 1*F*); 217 of these proteins were detected in both organs. Interestingly, the absolute counts of proteins satisfying these criteria (enriched in sieve elements, $P \leq 0.05$) were rather similar in stems (557) and leaves (639). Thus, the greater total number of proteins in stem as compared to leaf preparations seemed largely due to a greater variety of cell types in stem preparations. In other words, phloem preparations from leaves were "cleaner."

In samples from stems and leaves, 129 (2.0%) and 42 (1.2%) proteins, respectively, were detected in bulk phloem preparations but not in purified sieve elements. The opposite was true for 14 (0.2%) of the proteins in stem samples and 18 (0.5%) in samples from leaves. One might assume that proteins found exclusively in sieve element preparations were likely to possess sieve tube–specific functions. However, none of the proteins that appeared sieve element-exclusive in one organ (leaf or stem) was sieve element-exclusive also in the other. Half of the 32 proteins found exclusively in sieve element preparations from one

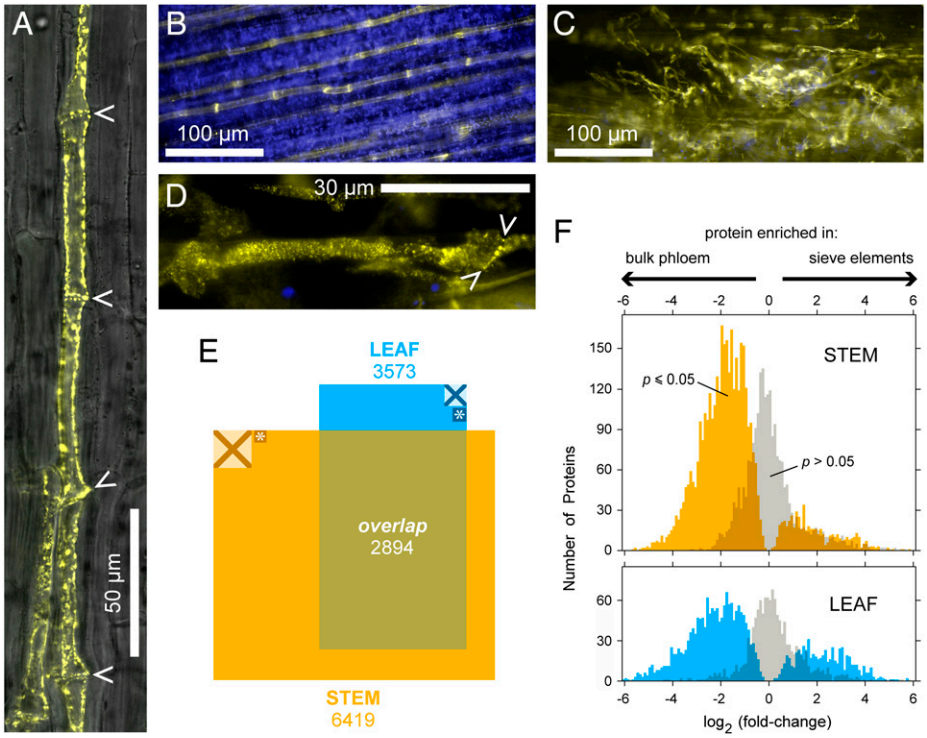

Fig. 1. Tissue preparation and proteomics analysis. (*A*) Functional sieve tube in a transgenic *N. tabacum* leaf with sieve elements specifically marked by fluorescence from ER-localized GFP (yellow; arrowheads: sieve plates). (*B*) Bulk phloem preparation from a stem, showing the sieve element–specific GFP signal (yellow) and chlorophyll autofluorescence (blue) originating from chloroplasts. (*C*) Purified sieve element preparation exhibiting strongly reduced chlorophyll fluorescence. (*D*) Individual sieve element in purified sample. A sieve plate is marked by arrowheads. (*E*) Protein diversity in preparations of phloem tissues from leaves and stems; rectangle areas correspond to protein numbers. Small squares with asterisks: proteins found in purified sieve element samples but not in bulk phloem; crossed squares: proteins found only in bulk phloem. All other proteins were detected in both bulk phloem and purified sieve elements. (*F*) Bar graphs visualizing the distribution of proteins between bulk phloem and purified sieve element preparations from stems (*Top*) and leaves (*Bottom*). Log_2 of the ratio of the amounts of each protein detected in sieve elements and bulk phloem (means of three biological replications) is indicated on the horizontal axis; each bar covers 0.1 of this parameter. Distributions of proteins for which the difference between sieve element and bulk phloem yielded $P \leq 0.05$ in Student's *t* test are shown in color; other proteins appear in gray.

of the two organs were not found at all in any samples, bulk phloem or purified sieve elements, from the other organ. Moreover, 24 of the 32 proteins were not present consistently in all three biological replicates. Thus, we concluded that the small proportion of proteins that were detected exclusively in sieve element preparations represented statistical noise rather than meaningful discoveries.

Distribution of Selected Proteins of Interest. Next, we evaluated the distributions of selected proteins between bulk phloem and purified sieve element preparations, starting with the sieve element–specific SEORs. Two tobacco SEORs, NtSEOR1 and -2, had been studied previously in living plants (42). However, the *N. tabacum* reference genome (41) has eight gene products annotated as "sieve element occlusion"(*SI Appendix*, Table S2), all sharing high sequence similarities with the two well-characterized SEORs of *Arabidopsis* (*SI Appendix*, Fig. S2). Our stem and leaf samples all contained six of the tobacco SEOR proteins, which were enriched in sieve element relative to bulk phloem preparations. In all but one case, the enrichment was 10-fold or larger (Fig. 2*A*). These results agreed with the cell biologically established sieve element–specific localization of SEORs. The reverse distribution pattern was expected for tubulins, as sieve elements lack microtubules. We detected the same three α-tubulins and two β-tubulins in all samples, with one and three additional β-tubulins present specifically in leaf and stem samples, respectively (*SI Appendix*, Table S3; classification of the tobacco tubulins was based on their similarities to *Arabidopsis* α- and β-tubulins; *SI Appendix*, Fig. S3). All tubulins were depleted in sieve element preparations compared to bulk phloem by factors between 0.69 and 0.12 (Fig. 2*A*).

A number of proteins exhibited comparable distribution patterns. For instance, we found six actin isoforms in our preparations (*SI Appendix*, Table S4 and Fig. S4), all of which were depleted in purified sieve elements (Fig. 2*B*) similarly as tubulins were (Fig. 2*A*). An example of a SEOR-like distribution was provided by the putative homologs of the callose synthase, CalS7 (GSL7). In *Arabidopsis*, this sieve element–specific enzyme is involved in generating the callose collars of sieve plate pores and thus in the regulation of the hydraulic resistance of sieve tubes (43, 44). Blasting its amino acid sequence against the *N. tabacum* protein database (41) identified a number of putative homologs. We detected seven of these proteins in our preparations, and two of them were accumulated in sieve elements like SEORs were (Fig. 2*B* and *SI Appendix*, Table S5). These two also were the most similar to AtCalS7 of all the putative homologs (*SI Appendix*, Fig. S5) and therefore appeared likely to represent functional equivalents of the *Arabidopsis* enzyme in *N. tabacum*. The presence in *N. tabacum* of two homologs of a single *Arabidopsis* protein was not surprising due to the allotetraploid character of the former species.

Potential problems of generalizing insights gained in *Arabidopsis* were exemplified by the 10 sucrose synthases (SuSy) present in all our leaf and stem samples (*SI Appendix*, Table S6). Two of the six isoforms known from *Arabidopsis*, SuSy5 and -6, recently were reported to occur exclusively in sieve elements of this species (45). Sequence comparison suggested one pair of the putative *N. tabacum* SuSys as homologs of each of the sieve

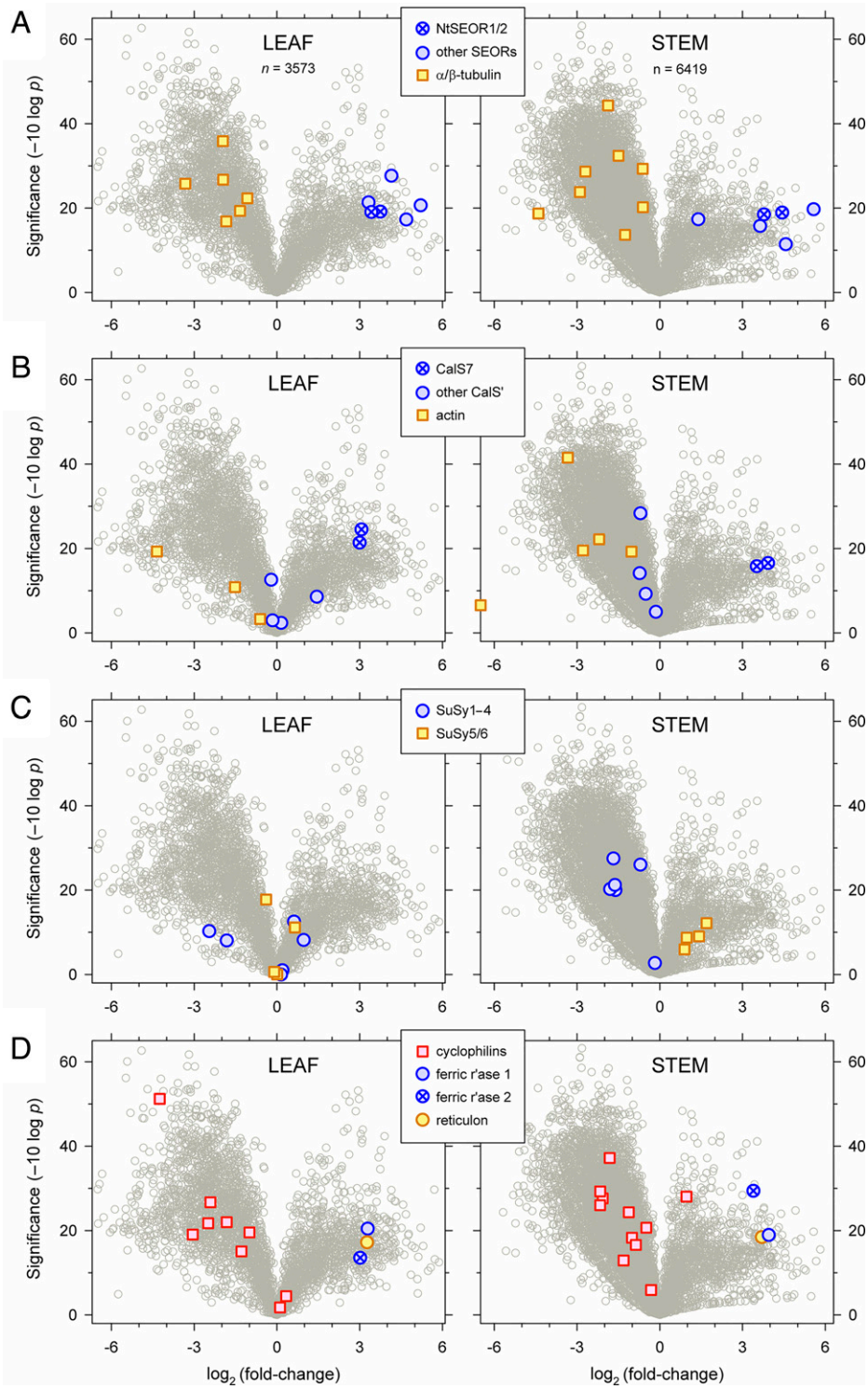

Fig. 2. Volcano plots visualizing the enrichment or depletion of proteins detected in purified sieve elements relative to bulk phloem preparations from leaves (n = 3,573; *Left*) and stems (n = 6,419; *Right*). Factors of enrichment or depletion (means of three biological replications) are presented on a logarithmic ($\log_2$) scale on the abscissae; ordinates show the statistical significance of the observed changes (as -10 log p, where p is derived from Student's t tests). (*A*) Typical distributions of proteins known exclusively from sieve elements (SEOR) and proteins without known function in these cells (tubulins). (*B*) Distributions of callose synthases (CalS; putative homologs of the sieve element–specific *Arabidopsis* CalS7 are highlighted) and actins. The datapoint plotted onto the vertical axis of the stem figure represents an actin isoform that was found only in bulk phloem preparations. (*C*) Organ-specific distributions of sucrose synthases (SuSy); putative homologs of the sieve element–specific Susy5 and -6 exhibit enrichment in purified sieve elements from stems but not leaves. (*D*) None of the putative homologs of reportedly phloem-specific CYPs from *B. napus* showed consistent enrichment in sieve elements. SEOR-like distributions were exhibited by two putative ferric reductases and one reticulon-like protein, which were further characterized cytologically.

element–specific AtSuSy5 and -6, while the other six tobacco proteins we had detected were more closely related to AtSuSy1 to 4 (*SI Appendix*, Fig. S6). Unexpectedly, none of the NtSuSys was significantly enriched in purified sieve elements compared to bulk phloem in leaf preparations (Fig. 2*C*). In stems, however, the putative homologs of AtSuSy1 to 4 and AtSuSy5/6 were depleted and enriched, respectively, in sieve elements (Fig. 2*C*). Statistically, the sieve element enrichment of each of the four AtSuSy5/6 homologs by itself was only weakly supported, but the overall pattern (Fig. 2*C*) was suggestive of an organ dependence of the tissue specificity of these proteins.

Cyclophilins (CYPs), ubiquitous proteins involved in a variety of cellular processes, provided an example of the general problems involved in assigning phloem-specific functions to proteins detected in potentially contaminated phloem exudates. In *Brassica napus*, a group of structurally similar CYPs had been found exclusively in phloem exudates, prompting the hypothesis that they served a specific and fundamental role in this tissue (46). Comparing the sequence of one of these proteins, BnCYP19-1, to the proteins in our samples, we identified a number of putative homologs (*SI Appendix*, Table S7). Almost all of these putative NtCYPs were significantly depleted in sieve element relative to bulk phloem preparations, while the only notable exception showed a significant but moderate twofold enrichment (Fig. 2*D* and *SI Appendix*, Table S7). This distribution, which resembled that observed for tubulin and actin, did not necessarily exclude a specific function of CYPs in sieve elements but was at least equally well in line with the idea that the presence of CYPs in sieve tube exudates was due to unspecific leakage from neighboring, nontransporting phloem cells into the translocation stream.

Confirmation of Sieve Element Specificity in Selected Proteins. Searching for potentially sieve element–specific proteins, we focused on cases with similar distribution patterns between bulk phloem and sieve element preparations as those observed for SEOR proteins and established a short list of promising candidates (*SI Appendix*, Table S1). We selected three proteins from this list, identified as Nitab4.5_0017493g0010.1, Nitab4.5_0020149g0010.1, and Nitab4.5_0000007g0250.1 in the reference database, which had never been characterized before. Uniprot domain searches revealed that the Nitab4.5_0017493g0010.1 protein (about 20 kDa) resembled reticulon-like proteins, while Nitab4.5_0020149g0010.1 (38 kDa) and Nitab4.5_0000007g0250.1 (45 kDa) were predicted to possess cytochrome b561/ferric reductase transmembrane domains. The distribution patterns of the reticulon-like protein and the putative ferric reductases 1 and 2 are shown in Fig. 2*D* (compare *SI Appendix*, Table S8).

To confirm that the three selected proteins were preferentially located in sieve elements, we transformed tobacco with constructs consisting of the endogenous promoter of the gene of interest (1,500 base pairs upstream of the coding region), the corresponding cDNA, and the sequence encoding the yellow fluorescent protein (YFP). The occurrence of YFP fluorescence in the transformed plants was observed by confocal microscopy. All three YFP-tagged proteins—putative ferric reductases 1 and 2, and the reticulon-like protein—were detected exclusively in sieve elements, where they were restricted to thin layers in the periphery of the cells (Fig. 3). The expression levels under the native promoters were weak in some lines. Especially in the lines producing the YFP-tagged reticulon-like protein, the fluorescence could not be seen with epifluorescence microscopes but was clearly detectable by confocal microscopy.

Subcellular Localization of Sieve Element–Specific Proteins. The peripheral localization of the three sieve element–specific proteins (Fig. 3) seemed to correspond to that reported for the ER in sieve elements. To see whether the proteins were in fact located in or at the ER, we crossed each of the three transgenic lines

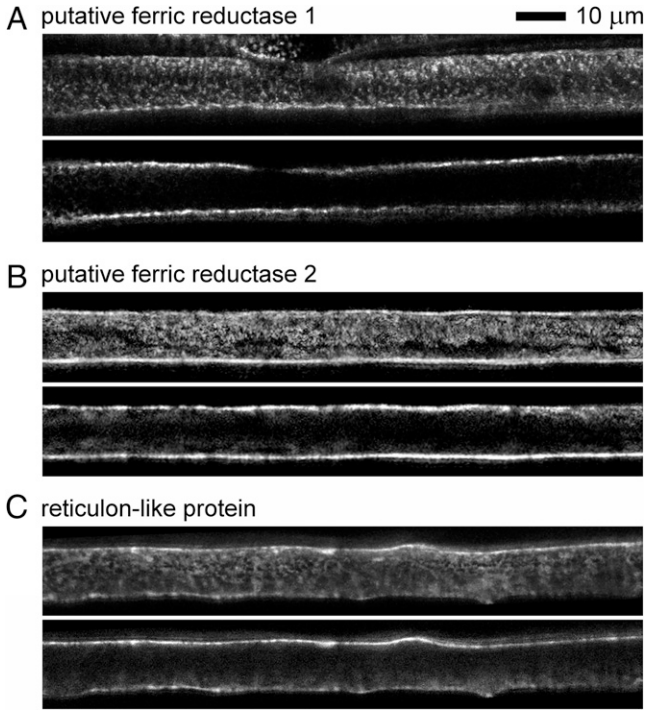

Fig. 3. Three sieve element–specific proteins are located predominantly in the periphery of mature sieve tubes. Transgenic *N. tabacum* producing YFP-tagged versions of either putative ferric reductase 1 (*A*), putative ferric reductase 2 (*B*), or reticulon-like protein (*C*) under the control of the native promoters showed YFP signals only in sieve elements (*Upper* micrographs in *A*, *B*, and *C*). Optical sections revealed that the signal originated almost exclusively from a thin peripheral layer in these cells (*Lower* micrographs in *A*, *B*, and *C*).

producing the YFP-tagged protein of interest with the pMtSEO2-HDEL-GFP line, in which the ER is marked specifically in sieve elements. The signal originating from the YFP-tagged putative ferric reductase 1 overlapped with the GFP signal from the ER only partly; numerous discrete foci were clearly separate from the ER (Fig. 4). Attempts to generate viable crosses producing YFP-tagged putative ferric reductase 2 together with GFP-tagged ER have remained unsuccessful so far, for unclear reasons. However, analogous crossing experiments with plants producing the YFP-tagged reticulon-like protein yielded similar results as with putative ferric reductase 1 (Fig. 5).

To further characterize the behavior of the proteins in live cells, we performed FRAP (fluorescence recovery after photobleaching) experiments. When we photobleached small rectangular zones in sieve elements exhibiting YFP fluorescence linked to the putative ferric reductase 1 and to the reticulon-like protein, no significant fluorescence recovery became evident over a period of 20 min (Fig. 6 *A* and *B*). Evidently, the diffusion of these two proteins was significantly restricted compared to that of the luminal HDEL-GFP, which showed complete fluorescence recovery in under 10 min (Fig. 6*C*).

Discussion

Since sieve elements are not amenable to analytical approaches based on analyses of gene activity, transcriptomics, or protein synthesis, we aimed at isolating sieve tubes to provide sufficient material for large-scale proteomics analyses of sieve elements. Among easily cultivated species with known whole-genome sequence data, *N. tabacum* proved the most suitable one for the manual isolation of phloem tissues from stems as well as leaves. Using a line expressing the GFP gene linked to the HDEL

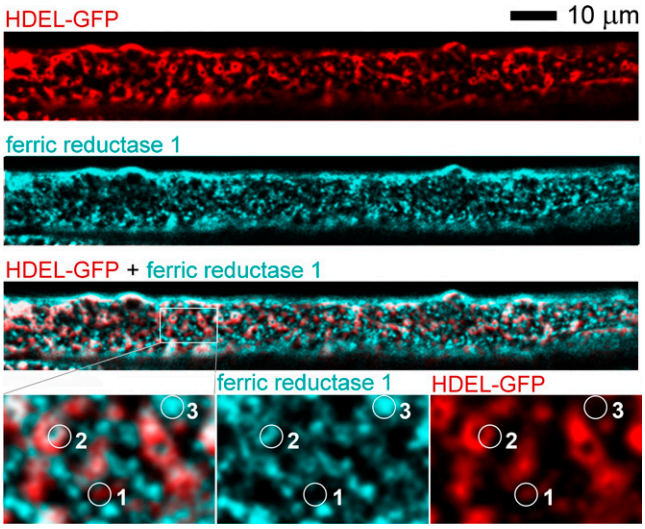

Fig. 4. The intracellular localization of a sieve element–specific putative ferric reductase does overlap with but is not restricted to the ER in transgenic *N. tabacum*. Dual fluorescence micrographs show the signals from the HDEL-GFP in the lumen of the ER and the YFP-tagged putative ferric reductase 1 in the same sieve element (*Top* and *Center*). The combined image (*Bottom*) confirms that the two signals (HDEL-GFP, red; ferric reductase 1, cyan) overlap partly (white). At higher magnification, it becomes evident that domains with exclusive HDEL-GFP signal (example in circle 1), domains with both signals (circle 2), and domains with exclusive ferric reductase 1-YFP signal in the ER (circle 3) exist.

ER-retention signal under the control of a sieve element–specific promoter (Fig. 1*A*) greatly facilitated quality control during the enzymatic isolation of the fluorescently marked sieve elements from bulk phloem (Fig. 1 *B*–*D*). We were able to produce purified sieve element samples with masses in the range of a few 10^{-5} g. Consequently, we could quantitatively compare the proteomes of bulk phloem and purified sieve elements, providing us with a criterion for selecting promising candidate proteins with sieve element–specific functions. This is a significant step forward from the microdissection method of Anstead et al. (32), who isolated bulk phloem from broccoli (*B. napus*) but did not purify sieve elements. Our simple protocol does not rely on complex preparative technologies and can be performed in any laboratory. In some contexts, this can be a decisive advantage over laser dissection (39, 40) and methods requiring the individual recognition of sieve element–derived protoplasts (47), for these approaches depend on advanced equipment and specialized skills to produce comparatively tiny amounts of materials for analysis.

The development of our enzymatic method, which degrades the walls of all cells but sieve elements, occurred by accident. In the context of a different project, we had attempted to produce sieve element protoplasts by exposing vascular tissues of *N. tabacum* to a standard cell wall–degrading enzyme mixture. The utter failure of this approach was the basis for the discovery of the purification technique for sieve elements presented here. While the underlying molecular mechanisms remain obscure, it is obvious that the composition and/or structure of sieve element cell walls differ in some important respect(s) from those of all neighboring cells.

Using the amino acid sequences predicted from the most recent genome sequences for *N. tabacum* (41), we identified thousands of proteins in bulk phloem and purified sieve element preparations from stems and leaves (Fig. 1*E* and Dataset S1). Evaluation of these data in terms of protein enrichment or depletion in purified sieve elements relative to bulk phloem yielded the expected results for the few proteins for which independent cytological information concerning their presence in sieve tubes was available. SEOR proteins are sieve element–specific P-proteins (12), and CalS7 is a sieve tube–specific callose synthase in *Arabidopsis* (43, 44). All six SEORs and the two apparent homologs of CalS7 included in our dataset of *N. tabacum* proteins were strongly enriched in purified sieve element samples from both stems and leaves (Fig. 2 *A* and *B*). In contrast, ubiquitous proteins without apparent function in sieve tubes such as the cytoskeletal components tubulin and actin were depleted in sieve tube samples from both organs (Fig. 2 *A* and *B*). The similarity of the distributions of actins and tubulins was in agreement with the reported absence of a functional actin cytoskeleton in sieve tubes (13) but not with claims to the opposite (48). We concluded that proteins showing distributions between bulk phloem and purified sieve element samples that resembled those of SEORs and CalS7 were likely to be sieve element-specific, leading us to select a short list of the most promising candidates (*SI Appendix*, Table S1).

On the other hand, we deliberately refrained from the usual large-scale in silico analyses of our set of detected proteins with respect to hypothetical protein function, predicted intracellular localization, putative binding partners, etc. Since only a vanishingly small proportion of the predicted proteins in tobacco plants has been characterized functionally and cytologically, almost all attributions of putative protein characters have to be deduced from sequence similarities with proteins from better known species, especially *Arabidopsis*. The assumptions involved in such an analysis are not unproblematic in the best case, and even more so in *N. tabacum*, a recently evolved allotetraploid (49). Due to increased rates of genome and gene evolution in polyploids (50, 51), the probability for a tobacco protein to not have the same physiological characteristics as its *Arabidopsis* homolog(s) must be expected to be comparatively high.

To highlight the validity of our approach, we here reported the first candidate proteins from our short list (*SI Appendix*, Table S1) for which we were able to generate transgenic tobacco plants expressing the YFP-tagged protein under the control of the native promoter. We had selected two of these proteins because they were annotated as possessing similarities to cytochrome b561/ferric reductases. Cytochromes b561 are membrane proteins involved in redox regulatory processes including ascorbate recycling and ion homeostasis (52–55). Functional

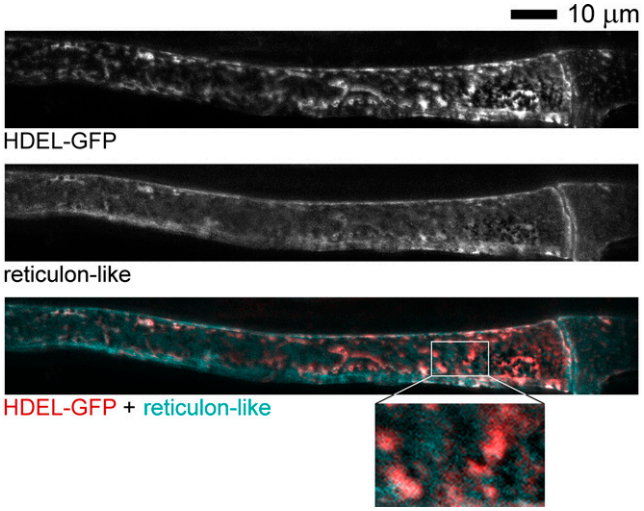

Fig. 5. The intracellular localization of a sieve element–specific reticulon-like protein overlaps only partly with the ER in transgenic *N. tabacum*. Dual fluorescence micrographs show the signals from the HDEL-GFP in the lumen of the ER and the YFP-tagged reticulon-like protein in the same sieve element (*Top* and *Center*). The combined image (*Bottom*) confirms that the overlap (white) of the two signals (HDEL-GFP, red; reticulon-like protein, cyan) is not complete. A sieve plate is visible on the *Right*.

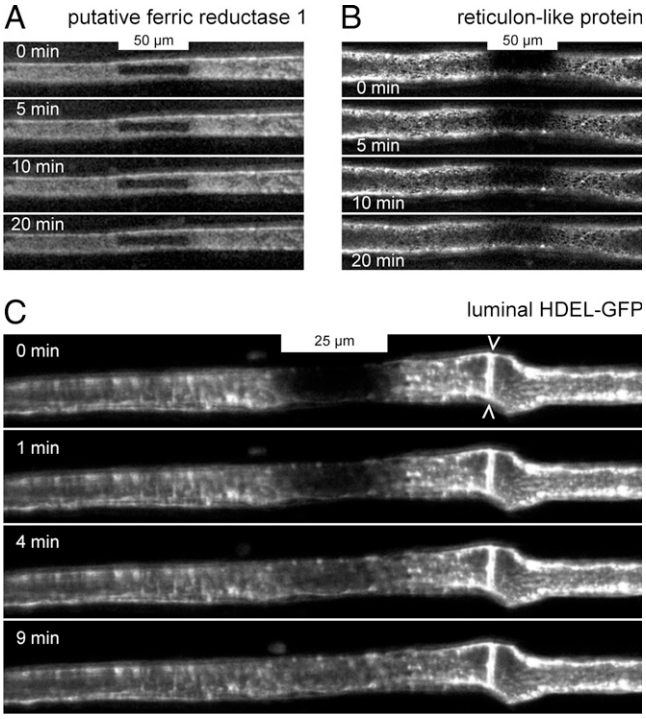

Fig. 6. FRAP experiments with sieve elements exhibiting fluorescence from YFP-tagged putative ferric reductase 1 (*A*), YFP-tagged reticulon-like protein (*B*), and GFP in the lumen of the ER (*C*; a sieve plate is marked by arrowheads). Rectangular fields (under the scale bars) were photobleached, and the recovery of the fluorescence was observed over 20 min. No or very weak recovery was detected over this period with the YFP-tagged proteins (*A* and *B*), while the signal from the luminal GFP recovered completely in under 10 min (*C*). Times marked on the images refer to the period that passed after the end of the photobleaching treatment. The tests shown are representative of at least four independent repetitions each.

phloem tissues experience very low oxygen levels and reducing redox potentials (56, 57). As a consequence, phloem-specific proteins are expected to be adapted to reducing conditions, and for forisomes, this has been experimentally verified (34). Sieve element–specific proteins potentially involved in redox regulation therefore appeared of particular interest. Both putative cytochrome b561/ferric reductases localized specifically to the periphery of sieve elements (Fig. 3 *A* and *B*). For one of them, we could directly show that its localization did not generally coincide with the ER, which also is restricted to a thin peripheral layer in these cells (Fig. 4). To explain these findings, we hypothesize that the peripheral endomembrane system of sieve elements is subdivided into two components (Fig. 7). First, the ER proper as identified in our transgenic plants by luminal GFP carrying the HDEL signal, a classical ER-retention sequence (58). Second, a (sub)compartment defined by the presence of a membrane protein, the sieve element–specific putative ferric reductase 1. This compartment seems to be connected to the ER proper (see zones of partially overlapping fluorescence signals in Fig. 4) but appears inaccessible to GFP diffusing in the ER lumen. The much reduced FRAP of the tagged putative ferric reductase 1 (Fig. 6*A*) indicates significant constraints on the diffusion of membrane components in the (sub)compartment characterized by this protein.

The ER is a polymorphic, highly dynamic structure. In plant cells, its mobility depends on the actin-myosin cytoskeleton (59). This implies severely reduced ER mobility in sieve elements, which lack actin filaments (13). On the other hand, the structural differentiation of the ER into tubular or sheet-like portions is at least partly independent of actin and requires reticulons, proteins that interact with the ER membrane (60, 61). Reticulons are abundant in plants (62) and are able to induce constrictions that restrict the diffusion of proteins in the ER (63, 64). Because reticulons could be responsible for the postulated differentiation of the ER, we further analyzed one of the two reticulon-like proteins included in our short list of promising candidates with sieve element–specific functions. The reticulon-like protein was clearly sieve element-specific and restricted to the cell periphery (Fig. 3*C*). Moreover, it showed reduced diffusivity in FRAP experiments (Fig. 6*B*), resembling the putative ferric reductase 1 in this respect. These findings could be explained by a revised working hypothesis, in which the inaccessibility of the second (sub)compartment for luminal GFP as well as the reduced diffusivity of membrane proteins in that (sub)compartment are interpreted as effects of reticulon action on the ER membrane (Fig. 7).

The ultrastructure of sieve elements deviates from the textbook stereotype of a plant cell and is difficult to study (11). Froelich et al. (65) described electron-dense vesicles in sieve tubes of *Arabidopsis* that seemed distinct from all known cellular compartments including the ER. It is tempting to speculate that these vesicles represent the compartment characterized by the presence of the putative ferric reductase 1 and/or the reticulon-like protein in tobacco. Unfortunately, the advanced preparation techniques for electron microscopy that were essential in discovering the unusual vesicles in *Arabidopsis* cannot easily be transferred to larger species such as *N. tabacum*, making it difficult to combine ultrastructural and molecular approaches to test the idea in tobacco. We can go the opposite way, though. The *Arabidopsis* genome includes 21 genes for reticulons (66). A single one of them, AtRTNLB9 (At3g18260), is by far the most similar of all *Arabidopsis* proteins to both reticulon-like proteins in our short list of potentially sieve element–specific *N. tabacum*

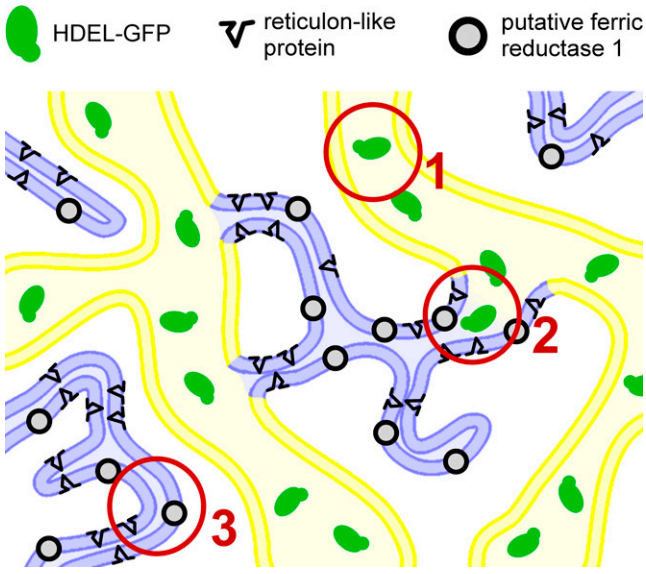

Fig. 7. Hypothetical explanation of the observations reported. The reduced endomembrane system of sieve elements consists of two parts (compare Fig. 4). First, the ER proper (yellow), which can be identified by fluorescence originating from GFP carrying the ER-retention signal HDEL (circle 1). Second, a previously uncharacterized compartment (blue) identifiable by fluorescence from YFP-tagged reticulon-like protein and putative ferric reductase 1 (circle 3). Generally, luminal GFP diffuses freely in the ER proper but is sterically excluded from the second compartment due to constrictions generated by reticulons acting on the organelle membrane. Transition zones, however, exist (circle 2). Redox enzymes such as the putative ferric reductase 1, which are involved in controlling the reducing redox potential in active sieve elements, are located in the membrane between the reticulons, where they experience reduced diffusivity. This model is to be understood as a simplifying working hypothesis intended to guide the next research steps.

proteins (*SI Appendix*, Table S1). The inference that AtRTNLB9 might be a sieve element–specific reticulon therefore is plausible. If corroborated, the whole battery of molecular, cell biological, and ultrastructural techniques established in the *Arabidopsis* model will become available for studying the unusual endomembrane system of sieve elements.

Due to the lack of a nucleus and translational machinery in sieve elements, and because of the difficulties to isolate sufficient amounts of these cells, only a handful of sieve tube–specific proteins have been functionally characterized. Consequently, the functions of major sieve element organelles such as the ER and the sieve element plastids have remained obscure. This is in stark contrast to other cell types. Here, we produced evidence suggesting a division of the sieve element ER into at least two subcompartments, distinguishable by characteristic, sieve element–specific proteins. This further emphasizes that sieve elements are far from being empty tubes. Our preparation protocols permit the identification of large numbers of highly enriched sieve element–specific proteins. As sieve tubes are involved in crucial physiological processes including plant/pathogen interactions, assimilate transport, long distance signaling, etc., our short list of sieve element–specific proteins (*SI Appendix*, Table S1) provides an exploratory tool that paves the way to a much clearer understanding of sieve tube biology.

Materials and Methods

Plant Material. Transgenic *N. tabacum* expressing GFP tagged to the sieve element endoplasmic reticulum under the control of the sieve element precursor–specific SEO2 promoter of *Medicago truncatula* was available in our laboratory (11). Wild-type and pMtSEO2-ER-GFP transgenic *N. tabacum* var. Petit Havana plants were maintained in a greenhouse at 25 °C with a 16/8-h photoperiod.

Preparation of Bulk Phloem and Purified Sieve Elements. To obtain phloem tissue from young, rapidly growing stems, the cortex was peeled exposing phloem on the inner side of the peel (*SI Appendix*, Fig. S1). The phloem was scratched off with scalpels or razor blades and sectioned into small fragments. Phloem from leaves was isolated from the midrib. When the midrib of a tobacco leaf is bent in the adaxial direction, the cortex cracks and can be peeled off to expose the phloem on the vascular bundle (*SI Appendix*, Fig. S1). The phloem layer can then be scratched off.

To isolate sieve elements from phloem tissues, samples were incubated overnight in 0.5% (wt/vol) cellulase Onozuka R-10 (Serva), 0.05% (wt/vol) pectolyase Y23 (Seishin Corp.), 0.5% (wt/vol) macerozyme R10 (Serva), 1% (wt/vol) bovine serum albumin (Sigma-Aldrich), 1 mM $CaCl_2$, and 10 mM Hepes/Tris (pH 5.6). The enzyme solution was adjusted to 800 mosmol · kg^{-1} with D-sorbitol (Sigma-Aldrich). This treatment preserved sieve element cell walls while the walls of all other cell types were digested. The resulting protoplast suspension was filtered through a nylon mesh (50 μm) and washed with 800 mM D-sorbitol and 1 mM $CaCl_2$. The remaining samples containing complete sieve elements were shock-frozen in liquid nitrogen, freeze-dried, and stored at room temperature.

Proteomics Analysis by Mass Spectrometry. The freeze-dried samples were denatured at 95 °C for 20 min in a buffer containing 2% SDS (sodium dodecyl sulfate), 50 mM Tris (pH 8.0), and 40 mM DTT (dithiothreitol). After samples had cooled to room temperature, 50 mM chloroacetamide were added for alkylation before samples were centrifuged to remove cell debris. The protein concentration in the supernatant was determined by SDS-PAGE (sodium dodecyl sulfate–polyacrylamide gel electrophoresis) followed by Coomassie staining. Up to 40 μg protein were extracted from the gel and washed with precooled 80% acetone. The proteins were dried and digested in 6 M urea and 50 mM Tris (pH 8.0) with 2 μg Lys-C protease at 37 °C for 3 h. The samples were digested further with 1 M urea, 50 mM Tris (pH 8.0), and 2 μg trypsin overnight, and then were acidified with 0.5% trifluoroacetic acid to stop the digestion reactions. The peptide mixtures were labeled with tandem mass tag multiplex kits (Thermo Fisher Scientific) for deep proteomic comparison. Quantitative liquid chromatography-mass spectroscopy (LC-MS/MS/MS, MS^3) analysis was performed with a nano-flow RP-HPLC (reversed-phase-high performance liquid chromatography) apparatus combined with a Tribrid Orbitrap Fusion mass spectrometer (Thermo Fisher Scientific); see *SI Appendix*, Table S9 for details. The datasets obtained were analyzed with PEAKS 8.5 (Bioinformatics Solutions Inc.).

Selection of Proteins of Potential Interest. Selection of proteins of interest among the 6,419 and 3,573 proteins unambiguously identified in stem and leaf samples, respectively (Dataset S1), proceeded in three steps. First, a statistical measure for the reliability of the protein identification provided by the PEAKS 8.5 software ("significance") was evaluated (67). Setting a threshold at 10 reduced the numbers of proteins from stems and leaves to 4,668 and 2,657, respectively. Second, using a fivefold enrichment factor in purified sieve elements compared to bulk phloem as a threshold further reduced the protein numbers to 237 and 320 in stems and leaves, respectively, with 123 proteins being present in samples from both organs. These 123 proteins were considered prime candidates for proteins with sieve element–specific functions (*SI Appendix*, Table S1).

Cloning and Design of Promoter–Reporter Constructs. Genomic DNA (gDNA) and cDNA sequences for the *N. tabacum* genes Nitab4.5_0017493g0010.1, Nitab4.5_0020149g0010.1, and Nitab4.5_0000007g0250.1 were obtained from the Solgenomics database (https://solgenomics.net); for amino acid sequences of the three proteins, see *SI Appendix*, Table S10. We selected 1,500-bp putative promoter sequences extending in the 5′ direction from but not including the translation start codons of the genes. The promoters were amplified from tobacco gDNA, and the cDNAs were amplified from a tobacco cDNA pool generated from RNAs extracted from sieve elements of wild-type tobacco plants. Promoter-cDNA-YFP constructs were generated using Gibson assembly (New England BioLabs), combining an amplified promoter, cDNA, and the YFP sequence with a linker in the binary vector AKK1426 containing a glufosinate resistance gene.

Stable Transformation of *N. tabacum*. Binary vectors used for stable plant transformation were introduced into *Agrobacterium tumefaciens* strain LBA4404 by the freeze–thaw method (68). Tobacco plants were transformed following established protocols (69).

Microscopy. The phloem in the midribs of leaves of transgenic plants expressing YFP-tagged, potentially sieve element–specific proteins was examined with a Leica SP8 confocal laser-scanning microscope (Leica Microsystems). YFP was excited with the 514-nm line of a white light laser, and emission was collected between 518 and 555 nm with a time gating setting of 0.3 to 5 ns. In case of weak fluorescence, a line accumulation between 6 and 12 was used to increase image quality. Images were processed with the Leica LAS AF Lite software and ImageJ (Fiji) version 1.52p (https://imagej.nih.gov/ij). FRAP was performed with the same settings . To bleach a specific area, the laser power was increased to 100% and the zoom was increased to 12× . After bleaching, the power was reduced to 10% and the zoom was set to 1× . An xyt movie was taken to document fluorescent protein diffusion. Imaging and FRAP experiments with GFP were performed with the 405-nm excitation line of a pulsed diode laser. The higher intensity of the laser allows faster bleaching, which is especially important for fast-diffusing probes. GFP emission was collected between 490 and 540 nm. Otherwise, the experiments were performed as described for YFP.

Data Availability. The mass spectrometry proteomics data have been deposited in the ProteomeXchange Consortium via the PRIDE partner repository with the dataset identifier PXD030457. All other relevant data are available within the article text and the supporting information.

ACKNOWLEDGMENTS. We thank the Franceschi Microscopy and Imaging Center at Washington State University for technical support. This work was supported by the US NSF (Grant No. 1940827).

1. R. F. Evert, Sieve tube structure in relation to function. *Bioscience* **32**, 789–795 (1982).
2. K. J. Oparka, R. Turgeon, Sieve elements and companion cells-traffic control centers of the phloem. *Plant Cell* **11**, 739–750 (1999).
3. M. Knoblauch, W. S. Peters, Long-distance translocation of photosynthates: A primer. *Photosynth. Res.* **117**, 189–196 (2013).
4. B.-K. Ham, W. J. Lucas, The angiosperm phloem sieve tube system: A role in mediating traits important to modern agriculture. *J. Exp. Bot.* **65**, 1799–1816 (2014).
5. H. D. Behnke, R. D. Sjolund, *Sieve Elements* (Springer, 1990).
6. A. J. E. van Bel, M. Knoblauch, Sieve element and companion cell: The story of the comatose patient and the hyperactive nurse. *Aust. J. Plant Physiol.* **27**, 477–487 (2000).
7. K. Esau, The Phloem *(Encyclopedia of Plant Anatomy, vol. 5)* (Borntraeger, 1969).
8. K. M. Furuta *et al.*, Plant development. *Arabidopsis* NAC45/86 direct sieve element morphogenesis culminating in enucleation. *Science* **345**, 933–937 (2014).

9. J.-O. Heo, B. Blob, Y. Helariutta, Differentiation of conductive cells: A matter of life and death. *Curr. Opin. Plant Biol.* **35**, 23–29 (2017).
10. D. D. Sabnis, H. M. Sabnis, "Phloem proteins: Structure, biochemistry and function" in *The Cambial Derivatives (Encyclopedia of Plant Anatomy)*, M. Iqbal, Ed. (Borntraeger, 1995), vol. **9**, part 4, pp. 271–292.
11. M. Knoblauch, W. S. Peters, Münch, morphology, microfluidics – Our structural problem with the phloem. *Plant Cell Environ.* **33**, 1439–1452 (2010).
12. M. Knoblauch, D. R. Froelich, W. F. Pickard, W. S. Peters, SEORious business: Structural proteins in sieve tubes and their involvement in sieve element occlusion. *J. Exp. Bot.* **65**, 1879–1893 (2014).
13. M. Knoblauch, W. S. Peters, K. Bell, T. J. Ross-Elliott, K. J. Oparka, Sieve-element differentiation and phloem sap contamination. *Curr. Opin. Plant Biol.* **43**, 43–49 (2018).
14. J.-Y. Kim *et al.*, Distinct identities of leaf phloem cells revealed by single cell transcriptomics. *Plant Cell* **33**, 511–530 (2021).
15. M. Knoblauch, K. Oparka, The structure of the phloem – Still more questions than answers. *Plant J.* **70**, 147–156 (2012).
16. R. Turgeon, The puzzle of phloem pressure. *Plant Physiol.* **154**, 578–581 (2010).
17. R. Turgeon, S. Wolf, Phloem transport: Cellular pathways and molecular trafficking. *Annu. Rev. Plant Biol.* **60**, 207–221 (2009).
18. A. Fischer, Ueber den Inhalt der Siebröhren der unverletzten Pflanze. *Ber. Deut. Bot. Ges.* **3**, 230–239 (1885).
19. M. Knoblauch, A. J. E. van Bel, Sieve tubes in action. *Plant Cell* **10**, 35–50 (1998).
20. J. Knoblauch, M. Knoblauch, V. V. Vasina, W. S. Peters, Sieve elements rapidly develop 'nacreous walls' following injury – A common wounding response? *Plant J.* **102**, 797–808 (2020).
21. S. Dinant, J. Kehr, "Sampling and analysis of phloem sap" in *Plant Mineral Nutrients: Methods and Protocols*, F. J. M. Maathuis, Ed. (Humana, 2013), pp. 185–194.
22. M.-K. Lin, Y.-J. Lee, T. J. Lough, B. S. Phinney, W. J. Lucas, Analysis of the pumpkin phloem proteome provides insights into angiosperm sieve tube function. *Mol. Cell. Proteomics* **8**, 343–356 (2009).
23. A. Barnes *et al.*, Determining protein identity from sieve element sap in *Ricinus communis* L. by quadrupole time of flight (Q-TOF) mass spectrometry. *J. Exp. Bot.* **55**, 1473–1481 (2004).
24. P. Giavalisco, K. Kapitza, A. Kolasa, A. Buhtz, J. Kehr, Towards the proteome of *Brassica napus* phloem sap. *Proteomics* **6**, 896–909 (2006).
25. C. Schobert *et al.*, Identification of immunologically related proteins in sieve-tube exudate collected from monocotyledonous and dicotyledonous plants. *Planta* **206**, 245–252 (1998).
26. C. Rodriguez-Medina, C. A. Atkins, A. J. Mann, M. E. Jordan, P. M. C. Smith, Macromolecular composition of phloem exudate from white lupin (*Lupinus albus* L.). *BMC Plant Biol.* **11**, 36 (2011).
27. B. Batailler *et al.*, Soluble and filamentous proteins in *Arabidopsis* sieve elements. *Plant Cell Environ.* **35**, 1258–1273 (2012).
28. G. Lattanzio *et al.*, Protein profile of *Lupinus texensis* phloem sap exudates: Searching for Fe- and Zn-containing proteins. *Proteomics* **13**, 2283–2296 (2013).
29. A. Ostendorp *et al.*, Functional analysis of *Brassica napus* phloem protein and ribonucleoprotein complexes. *New Phytol.* **214**, 1188–1197 (2017).
30. C. Zhang, X. Yu, B. G. Ayre, R. Turgeon, The origin and composition of cucurbit "phloem" exudate. *Plant Physiol.* **158**, 1873–1882 (2012).
31. K. J. Oparka, S. S. Cruz, THE GREAT ESCAPE: Phloem transport and unloading of macromolecules. *Annu. Rev. Plant Physiol. Plant Mol. Biol.* **51**, 323–347 (2000).
32. J. A. Anstead, S. D. Hartson, G. A. Thompson, The broccoli (*Brassica oleracea*) phloem tissue proteome. *BMC Genomics* **14**, 764 (2013).
33. W. S. Peters, M. Knoblauch, S. A. Warmann, W. F. Pickard, A. Q. Shen, Anisotropic contraction in forisomes: Simple models won't fit. *Cell Motil. Cytoskeleton* **65**, 368–378 (2008).
34. M. Knoblauch, M. Stubenrauch, A. J. E. van Bel, W. S. Peters, Forisome performance in artificial sieve tubes. *Plant Cell Environ.* **35**, 1419–1427 (2012).
35. H. C. Pélissier, W. S. Peters, R. Collier, A. J. E. van Bel, M. Knoblauch, GFP tagging of sieve element occlusion (SEO) proteins results in green fluorescent forisomes. *Plant Cell Physiol.* **49**, 1699–1710 (2008).
36. W. S. Peters, D. Haffer, C. B. Hanakam, A. J. E. van Bel, M. Knoblauch, Legume phylogeny and the evolution of a unique contractile apparatus that regulates phloem transport. *Am. J. Bot.* **97**, 797–808 (2010).
37. D. L. Mullendore *et al.*, Non-dispersive phloem-protein bodies (NPBs) of *Populus trichocarpa* consist of a SEOR protein and do not respond to cell wounding and Ca^2. *PeerJ* **6**, e4665 (2018).
38. J. A. Anstead, D. R. Froelich, M. Knoblauch, G. A. Thompson, *Arabidopsis* P-protein filament formation requires both AtSEOR1 and AtSEOR2. *Plant Cell Physiol.* **53**, 1033–1042 (2012).
39. B. Zhang, V. Tolstikov, C. Turnbull, L. M. Hicks, O. Fiehn, Divergent metabolome and proteome suggest functional independence of dual phloem transport systems in cucurbits. *Proc. Natl. Acad. Sci. U.S.A.* **107**, 13532–13537 (2010).
40. R. M. Lopez-Cobollo, I. Filippis, M. H. Bennett, C. G. N. Turnbull, Comparative proteomics of cucurbit phloem indicates both unique and shared sets of proteins. *Plant J.* **88**, 633–647 (2016).
41. K. D. Edwards *et al.*, A reference genome for *Nicotiana tabacum* enables map-based cloning of homeologous loci implicated in nitrogen utilization efficiency. *BMC Genomics* **18**, 448 (2017).
42. A. M. Ernst *et al.*, Sieve element occlusion (SEO) genes encode structural phloem proteins involved in wound sealing of the phloem. *Proc. Natl. Acad. Sci. U.S.A.* **109**, E1980–E1989 (2012).
43. B. Xie, X. Wang, M. Zhu, Z. Zhang, Z. Hong, *CalS7* encodes a callose synthase responsible for callose deposition in the phloem. *Plant J.* **65**, 1–14 (2011).
44. D. H. P. Barratt *et al.*, Callose synthase GSL7 is necessary for normal phloem transport and inflorescence growth in *Arabidopsis*. *Plant Physiol.* **155**, 328–341 (2011).
45. D. Yao, E. Gonzales-Vigil, S. D. Mansfield, *Arabidopsis* sucrose synthase localization indicates a primary role in sucrose translocation in phloem. *J. Exp. Bot.* **71**, 1858–1869 (2020).
46. P. Hanhart *et al.*, Bioinformatic and expression analysis of the *Brassica napus* L. cyclophilins. *Sci. Rep.* **7**, 1514 (2017).
47. J. B. Hafke, A. C. U. Furch, M. U. Reitz, A. J. E. van Bel, Functional sieve element protoplasts. *Plant Physiol.* **145**, 703–711 (2007).
48. J. B. Hafke *et al.*, Involvement of the sieve element cytoskeleton in electrical responses to cold shocks. *Plant Physiol.* **162**, 707–719 (2013).
49. I. J. Leitch *et al.*, The ups and downs of genome size evolution in polyploid species of *Nicotiana* (Solanaceae). *Ann. Bot.* **101**, 805–814 (2008).
50. J. F. Wendel, Genome evolution in polyploids. *Plant Mol. Biol.* **42**, 225–249 (2000).
51. S. P. Otto, The evolutionary consequences of polyploidy. *Cell* **131**, 452–462 (2007).
52. M. Tsubaki, F. Takeuchi, N. Nakanishi, Cytochrome b561 protein family: Expanding roles and versatile transmembrane electron transfer abilities as predicted by a new classification system and protein sequence motif analyses. *Biochim. Biophys. Acta* **1753**, 174–190 (2005).
53. A. Bérczi, D. Su, H. Asard, An *Arabidopsis* cytochrome b561 with trans-membrane ferrireductase capability. *FEBS Lett.* **581**, 1505–1508 (2007).
54. H. Asard, R. Barbaro, P. Trost, A. Bérczi, Cytochromes *b*561: Ascorbate-mediated trans-membrane electron transport. *Antioxid. Redox Signal.* **19**, 1026–1035 (2013).
55. A. Bérczi, L. Zimányi, The *trans*-membrane cytochrome *b*561 proteins: Structural information and biological function. *Curr. Protein Pept. Sci.* **15**, 745–760 (2014).
56. M. J. Darwent, W. Armstrong, J. Armstrong, P. M. Beckett, Exploring the radial and longitudinal aeration of primary maize roots by means of Clark-type oxygen microelectrodes. *Russ. J. Plant Physiol.* **50**, 808–820 (2003).
57. J. T. van Dongen, U. Schurr, M. Pfister, P. Geigenberger, Phloem metabolism and function have to cope with low internal oxygen. *Plant Physiol.* **131**, 1529–1543 (2003).
58. V. Gomord *et al.*, The C-terminal HDEL sequence is sufficient for retention of secretory proteins in the endoplasmic reticulum (ER) but promotes vacuolar targeting of proteins that escape the ER. *Plant J.* **11**, 313–325 (1997).
59. I. Sparkes, C. Hawes, L. Frigerio, FrontiERs: Movers and shapers of the higher plant cortical endoplasmic reticulum. *Curr. Opin. Plant Biol.* **14**, 658–665 (2011).
60. G. K. Voeltz, W. A. Prinz, Y. Shibata, J. M. Rist, T. A. Rapoport, A class of membrane proteins shaping the tubular endoplasmic reticulum. *Cell* **124**, 573–586 (2006).
61. J. Hu *et al.*, Membrane proteins of the endoplasmic reticulum induce high-curvature tubules. *Science* **319**, 1247–1250 (2008).
62. T. Oertle, M. Klinger, C. A. O. Stuermer, M. E. Schwab, A reticular rhapsody: Phylogenic evolution and nomenclature of the *RTN/Nogo* gene family. *FASEB J.* **17**, 1238–1247 (2003).
63. N. Tolley *et al.*, Overexpression of a plant reticulon remodels the lumen of the cortical endoplasmic reticulum but does not perturb protein transport. *Traffic* **9**, 94–102 (2008).
64. I. Sparkes *et al.*, Five *Arabidopsis* reticulon isoforms share endoplasmic reticulum location, topology, and membrane-shaping properties. *Plant Cell* **22**, 1333–1343 (2010).
65. D. R. Froelich *et al.*, Phloem ultrastructure and pressure flow: Sieve-element-occlusion-related agglomerations do not affect translocation. *Plant Cell* **23**, 4428–4445 (2011).
66. H. Nziengui *et al.*, Reticulon-like proteins in *Arabidopsis thaliana*: Structural organization and ER localization. *FEBS Lett.* **581**, 3356–3362 (2007).
67. PEAKS Team, PEAKS 8.5 User Manual (2017). https://www.bioinfor.com/user-manual/. Accessed 10 July 2021.
68. H. Chen, R. S. Nelson, J. L. Sherwood, Enhanced recovery of transformants of *Agrobacterium tumefaciens* after freeze-thaw transformation and drug selection. *Biotechniques* **16**, 664–668, 670 (1994).
69. G. An, High efficiency transformation of cultured tobacco cells. *Plant Physiol.* **79**, 568–570 (1985).